Superconducting states as quantum bits

Tzu-Chieh Wei

Department of Physics, University of Illinois at Uranba-Champaign, Illinois 61801, USA
(Dated: May 6, 2002)

Abstract

There are two basic types of proposals of superconductors used to implement quantum bits (qubits): flux qubits and charge qubits. These two designs are based on Josephson junction but are operated at two extreme regimes: phase dominated and charge dominated regimes respectively. In both limits, the system behaves approximately as a two-level quantum-mechanical system, which serves as a basic requirement of quantum bits. There is a recent hybrid design, which can operate at the intermediate regime under appropriate control. In this paper, we focus on discussions of these designs of qubits and experiments demonstrating coherent superpositions of two levels and coherent control of some systems, with the problems regarding decoherence and measurement briefly mentioned in the concluding remarks.

I. INTRODUCTION

Quantum computer[1, 2] that promises us to perform powerful tasks, such as fast factoring long-digit numbers and efficiently searching an item out of a large unsorted database, can only be theorists' dream if no physical system can reliably implement proposed quantum algorithms. The delicate manipulation of quantum states is susceptible to the disturbance from the environment, so called the decoherence. The quantum system must[3] have well-defined quantum states, usually two-level (thereby termed quantum bits), in which arbitrary superposition is possible and long-lived. Also, in order to perform operation, we must be able to prepare some initial states of all the quantum bits (qubits), precisely control the state of each qubit and interactions with other qubits, and finally read out the states of specific qubits at the end of "computation". Also, from the technological point of view, we need to put a large number of qubits together into manufacture.

Superconductors with Josephson junctions offer one of the most promising playgrounds for realizing quantum computation, since, the fabrication technology is very matured, and under appropriate conditions, the superconducting system can behave as a well-defined two-level system, and some coherent control over the two levels have already been demonstrated. The two levels are usually macroscopically different, in that there are a macroscopical number of Cooper pairs collectively acting coherently, e.g. circulating in one direction of a superconducting loop for one state and in the opposite direction for the other. Being able to build a superposition of macroscopically different states also offers an insight into the fundamental problems [4] of quantum mechanics itself, e.g. , the validity of quantum mechanics applying to everyday objects without any modification and the measurement problem as distinct process to unitary evolution.

The study of superconducting systems to implement qubits is thus both fundamentally and quantum computationally interesting. There are three different types of designs so far: charge qubit, flux qubit, and "quantronium" (which operates in the intermediate regime of the former two). In this Paper, we review each of the three designs and related experiments[15] in Sec. III, Sec. IV, and Sec. V respectively. Finally, we make some concluding remarks in Sec. VI.

II. JOSEPHSON EFFECT

We start by discussing the Josephson effect[16], since Josephson junction is the most important element in designing superconducting qubits. Suppose there are two superconducting electrodes connected by a weak link, which can be an insulating layer, a normal metal layer, or a narrow constriction. The two superconducting electrodes can be described by a Landau-Ginzburg wavefunction $\psi_j = |\psi_j|e^{i\phi_j}$. Josephson found that, at zero bias voltage, there is a supercurrent flowing between the two electrodes, i.e., $I_s = I_c \sin \Delta\phi$, where $\Delta\phi$ is the phase difference and I_c is the critical current, i.e., the maximal supercurrent the junction can support. Furthermore, if a nonzero bias voltage V is maintained across the junction, the supercurrent will be alternating with the phase difference given by $\Delta\phi = \Delta\phi_0 + 2eVt/\hbar$. The free energy stored in the junction can be drived

$$F = \int VI_s dt = \text{const.} - E_J \cos \Delta\phi, \tag{1}$$

where $E_J \equiv \hbar I_c/2e$ is the Josephson coupling energy. In the presence of a vector potential A, we can employ gauge transformation to derive the equation for supercurrent. Suppose $\psi = |\psi|e^{i\phi}$ is the solution to the Landau-Ginzburg (LG) equation in the absence of the vector potential $A = 0$, and $\psi' = |\psi'|e^{i\phi'}$ is the corresponding solution in the presence of A, the two solutions are connected by,

$$\psi' = |\psi'|e^{i\phi'} = \psi \exp\left(i\frac{2\pi}{\Phi_0} \int \mathbf{A} \cdot d\mathbf{s}\right), \tag{2}$$
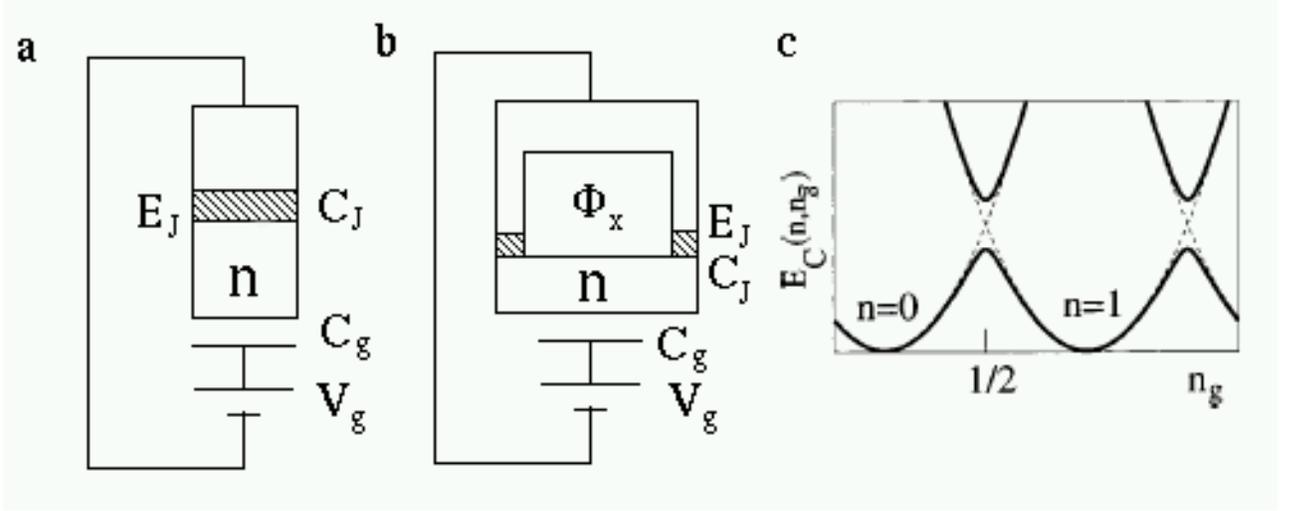
FIG. 1: Josephson charge qubits: (a) The simplest design. (b) Replace the junction in (a) by a loop with two junctions. (c) The total charging energy as a function of n_g.

as can be easily seen from the LG equation: $\alpha\psi + \beta|\psi|^2\psi + (1/2m^*)(\hbar/i\nabla - 2eA/c)^2\psi = 0$, in which

$$(\frac{\hbar}{i}\nabla - \frac{2e}{c}A)^2\left(\psi\exp(i\frac{2\pi}{\Phi_0}\int \mathbf{A}\cdot d\mathbf{s})\right) = \exp(i\frac{2\pi}{\Phi_0}\int \mathbf{A}\cdot d\mathbf{s})(\frac{\hbar}{i}\nabla)^2\psi, \tag{3}$$

where $\Phi_0 \equiv hc/2e$ is the flux quantum, and the line integral starts from some arbitray reference point. Thus, we can define a gauge-invariant phase differnce: $\gamma \equiv \Delta\phi' - (2\pi/\Phi_0)\int_1^2 \mathbf{A}\cdot d\mathbf{s}$, where the line integral starts from one superconducting electrode to the other, and the supercurrent in the Josephson junction, in terms of the gauge-invariant phase difference, becomes $I_s = I_c\sin\gamma$. The free energy of a Josephson junction in the presence of a gauge potential is, therefore,

$$F = \text{const.} - E_J\cos\gamma. \tag{4}$$

III. CHARGE QUBIT

Fig. 1a shows a simplest design of qubit, usually called Cooper pair box, in which a superconductor island (with execess charge Q) is connected ,at one end, through a Josephson junction (with shunt capacitance C_J), to a superconducting electrode biased at zero voltage, and, at the other end, to a voltage source V_g through a capacitor C_g. There are several contributions to the Hamiltonian. In addition to the tunneling energy discussed previously in Eq. (4), we have to take into account energy stored in the two capacitors C_g and C_J. Suppose there is an excess of charge Q (relative to neutral state) on the superconducting island, and the charges on the two capacitors are q_1 and q_2 respectively. The potential V of the island can be easily computed from the relations

$$q_1 = C_g(V_g - V), \ q_2 = C_J(0 - V), \ q_1 + q_2 + Q = 0, \tag{5}$$

and we have $V = (C_gV_g + Q)/(C_g + C_J)$. The electrostatic energy is then

$$U = \sum_i \frac{1}{2}C_i(V_i - V)^2 = \frac{1}{2C_\Sigma}(Q^2 + C_JC_gV_g^2), \tag{6}$$

where we define $C_\Sigma \equiv C_g + C_J$ to be the sum of the two capacitors. But this is not all. We also have to subtract the energy supplied by the voltage source when the charge tunnels (through the
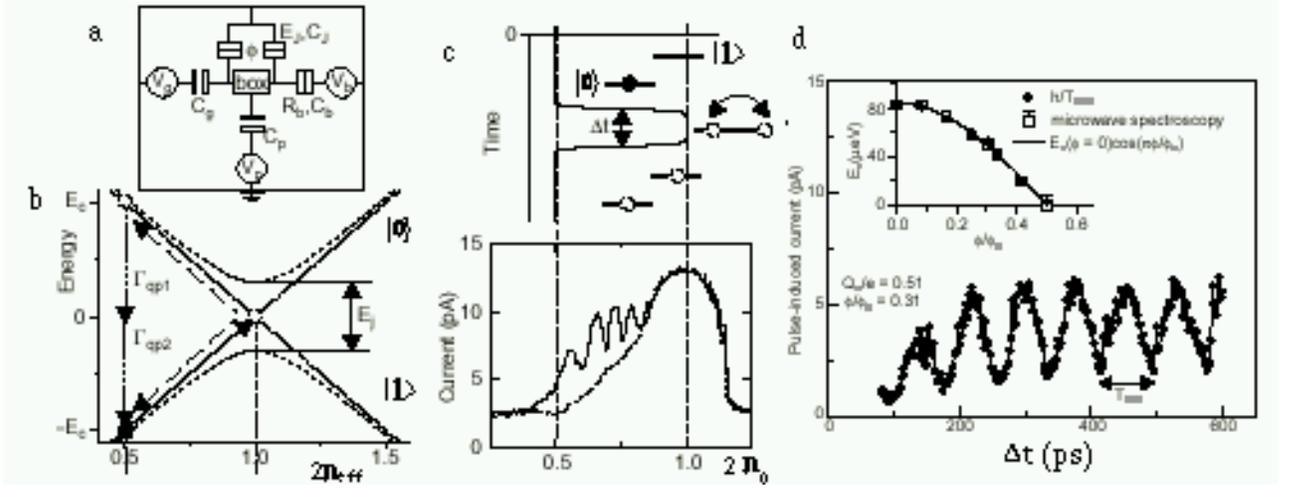
3

FIG. 2: Coherent control of quantum states in a Cooper pair box.

junction) into the island. Suppose an electron tunnels in, this changes the potential V by e/C_Σ, resulting changes of charges on each capacitor by $-eC_g/C_\Sigma$ and $-eC_J/C_\Sigma$ respectively. Hence the work done by the voltage source (V_g) is $-eC_gV_g/C_\Sigma$. After total charge Q tunnels in, the total work done by the voltage source is $W = -(QC_gV_g)/C_\Sigma$[17]. Therefore, the total energy E is

$$E = F + U - W = \frac{1}{2C_\Sigma}(Q + C_gV_g)^2 - E_J\cos\Delta\phi + \frac{1}{2}C_gV_g^2(\frac{C_J - C_g}{C_\Sigma}), \tag{7}$$

where the last term independent of Q can be ignored. If the energy gap Δ of the superconductor is much larger than the charging energy $E_c \equiv e^2/2C_\Sigma$, single electron tunneling is suppressed, and thus the excess charge ($Q = 2ne$) can only exist in the form of Cooper pairs. The resulting Hamiltonian is then

$$\mathcal{H} = 4E_C(n - n_g)^2 - E_J\cos\Theta, \tag{8}$$

where $n_g = -C_gV_g/2e$ is the effective number of charge pair due to the gate voltage and Θ is the phase of the superconductor island (taking that of superconducting electrode to be zero). Furthermore, if the charging energy E_C is much larger than the Josephson coupling energy E_J, the convenient basis to describe the Hamiltonian is n instead of Θ. Using the relation $e^{\pm i\Theta}|n\rangle = |n \pm 1\rangle$, as can be understood in the correspondence $(\Theta, n) \leftrightarrow (\hat{x}, \hat{p})$, where the latter set satisfies $e^{ik\hat{x}}|p\rangle = |p + k\rangle$, we arrive at the expression for the Hamiltonian

$$\mathcal{H} = \sum_n \left\{ 4E_C(n - n_g)^2|n\rangle\langle n| - \frac{1}{2}E_J\big(|n\rangle\langle n + 1| + |n + 1\rangle\langle n|\big) \right\}. \tag{9}$$

We plot in Fig. 1c the "potential" term as a function of n_g, taking into account possible mixing. We see when V_g is biased such that n_g is close to, say, $1/2$, the two nearby states $|0\rangle$ and $|1\rangle$ are degenerate and can be mixed by the Josephson term. Near this degenerate point, the Hamiltonian can be approximated as

$$\mathcal{H} \approx 4E_C\big(n_g^2|0\rangle\langle 0| + (1 - n_g)^2|1\rangle\langle 1|\big) - \frac{1}{2}(|0\rangle\langle 1| + |1\rangle\langle 0|) \tag{10}$$

$$= 4E_C\begin{pmatrix} (n_g - \frac{1}{2}) & 0 \\ 0 & -(n_g - \frac{1}{2}) \end{pmatrix} + 2E_C(2n_g^2 - 2n_g + 1)\begin{pmatrix} 1 & 0 \\ 0 & 1 \end{pmatrix} + \frac{1}{2}E_J\begin{pmatrix} 0 & 1 \\ 1 & 0 \end{pmatrix}, \tag{11}$$

where the second term is a constant term (even if n_g changes with time, the effect on any state is still same) and can be ignored. In terms of Pauli matrices, $\mathcal{H}$ becomes

$$\mathcal{H} = -\frac{1}{2}B_z\sigma_z - \frac{1}{2}B_x\sigma_x, \tag{12}$$
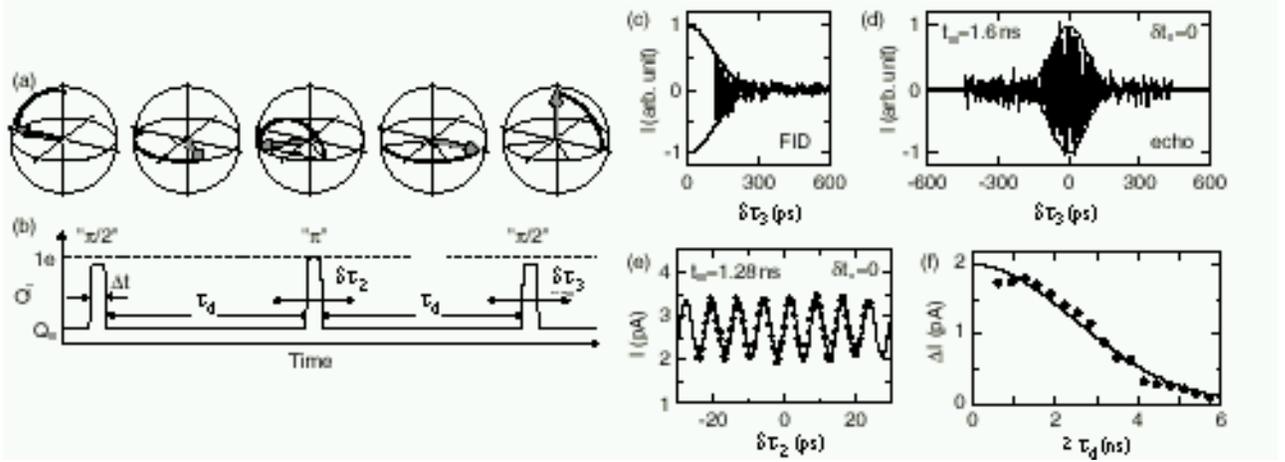
4

FIG. 3: The charge echo experiment.

where $B_z \equiv 4E_c(1 - 2n_g)$ and $B_x \equiv E_J$.

If we replace the junction by a low-self-conductance SQUID (Fig. 1 b) threaded by flux Φ_x, the potential $-E_J \cos \Theta$ changes to $-\tilde{E}_J(\Phi_x) \cos \Theta$, where $\tilde{E}_J(\Phi_x) = 2E_J \cos(\pi\Phi_x/\Phi_0)$ (see Sec. IV) , and the resulting B_z and B_x are independently controllable by V_g and Φ_x respectively. Arbitrary single-qubit operation (rotation) can be achieved by controlling B_z and B_x.

A. The NEC Experiments

In addition to the design shown in Fig. 1b, the experimental setup[5–7] in the NEC group has two other voltage sources: V_p (with capacitor C_p) for applying a pulsed voltage to bring the system to the degenerate point and V_b (with capacitor C_b) biased such that the one-pair-execess state $|1\rangle$ will decay to state $|0\rangle$ by two sequential quasiparticle tunneling events through the probe junction; see Fig. 2a.

The effective bias pair number n_{eff} (n_g in previous section), is now determined by the three voltage sources: $n_{\text{eff}} = (C_g V_g + C_b V_b + C_p V_p(t))/2e = n_0 + C_p V_p(t)/2e$, where we define $n_0 \equiv (C_g V_g + C_b V_b)/2e$. Fig. 2b shows the energy levels near $2n_{\text{eff}} = 1$ and a schematic evolution of the state $|0\rangle$ initially far from the degeneracy point. As the pulse voltage V_p is on for a short interval Δt (see Fig. 2c), the system is brought to the neighborhood of the degeneracy point, at which the state $|0\rangle$ can tunnel into state $|1\rangle$ by mixing, and subsequently decay back into $|0\rangle$ by the sequential tunneling of electrons through the probe junction. The current flows through the probe is proportional to, and thus a measure of, the probability of the transition $|0\rangle \to |1\rangle$. Fig. 2c compares the results to the case when no pulse is applied (there can still be sequential quasiparticle tunneling), and it shows the oscillation of the transition probability as a function of n_0 and has the highest peak at $n_0 = 0.5$.

Furthermore, they also start the experiment with a fixed value of $2n_0 = 0.51$, apply a pulse voltage such that $2n_p = C_p V_p/e = 0.49$ for a duration Δt, during which the system is at degeneracy point $2n_{\text{eff}} = 1$, and measure the pulse-induced current after the pulse is off. In view of Eq. (12), when the pulse is on, $B_z = 4E_c(1 - 2n_{\text{eff}}) = 0$, the evolution becomes a "spin rotation" in x-direction

$$e^{i\Delta t B_x \sigma_x/2} = \begin{pmatrix} \cos(\Delta t B_x/2) & i\sin(\Delta t B_x/2) \\ i\sin(\Delta t B_x/2) & \cos(\Delta t B_x/2) \end{pmatrix}. \tag{13}$$

The probability of $0 \to 1$ transition is $P(1; \Delta t) = \sin^2(\Delta t B_x/2)$ if initially the state is in $|0\rangle$. They observe such oscillation in the induced current (Fig. 2d), and determine the period $T_{\text{coh}} \equiv 2\pi/B_x = 2\pi/\tilde{E}_J$ experimentally. They repeat the same procedure for different values of $\tilde{E}_J$ (controllable by Φ_x) and agree with the results from microwave spectroscopy[6].
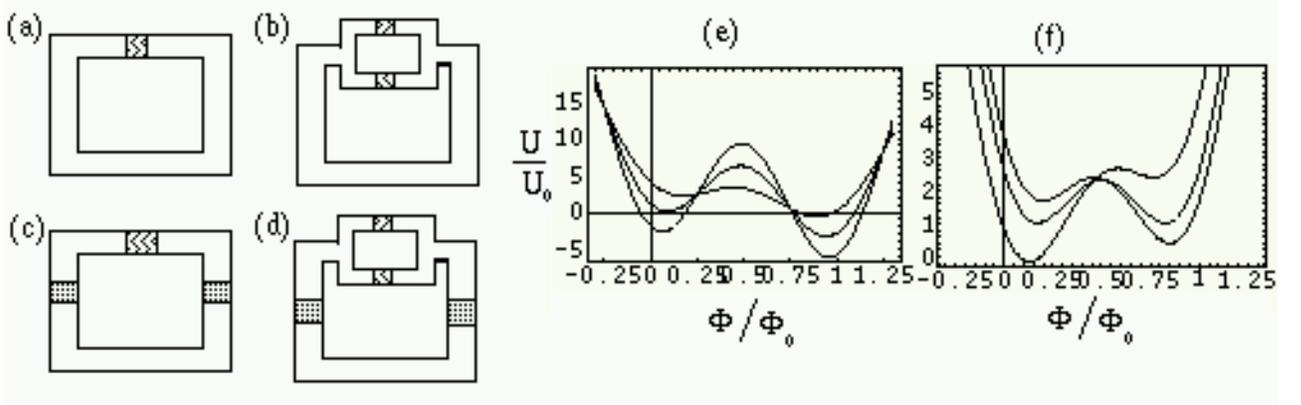
5

FIG. 4: (a)-(d) Several variations of flux qubits. (e)(f) The potential $U(\Phi)/U_0$ versus Φ/Φ_0. In (e), $\Phi_{\text{ext}}/\Phi_0 = 0.6$ and the corresponding β_L are 9,6,3 respectively as we go from top to bottom curves along the central barrier. In (d), $\beta_L = 2.33$, and Φ_{ext}/Φ_0 are 0.4, 0.5, and 0.55 respectively as we go from top to bottom curves along the right well.

The same group recently demonstrates coherent control of single-qubit rotations in a "charge echo" experiment [7], in that it is the charge rather than spin state that is rotated on the Bloch sphere, as is easily seen from the equivalence of the system Hamiltonian to that of a spin-1/2. The schematic rotations are shown in Fig. 3a, where we see that no matter what the position of the arrow (indicating the "spin" direction) on the equator is time τ_d after the first $\pi/2$ x-rotation, after a π x-rotation followed by the same duration τ_d, the arrow should end up at the same position. The corresponding applied voltage pulse sequence is shown in Fig. 3b, and the final $\pi/2$ pulse is used to rotate the state back to $|0\rangle$ and $|1\rangle$ for the purpose of measuring the transition current in the probe junction. This refocusing technigue can be used to eliminate low frequency fluctuations (some arrows lie a little bit ahead and some behind), so that the different arrows remain coherent with respect to each other. A small delay in the second rotation (π) and third rotation ($\pi/2$) will result in oscillation of the induced current, while longer delay will result in decay of the signal as well; see Figs. 3de. Fig. 3f shows the decay time of the signal with this correctional procedure as compared to that without in Fig 3d, and we see that the decay time is indeed enhanced. The important message from this experiment is that the coherent control of single charge-qubit operations have been demonstrated.

IV. FLUX QUBIT

The simplest flux qubit is made up of a superconducting loop with a Josephson junction (Fig. 4a). We first derive the Hamiltonian in terms of total flux threaded through the loop. Recall that the supercurrent velocity is given by

$$\mathbf{v}_s = \frac{1}{m^*}(\mathbf{p}_s - \frac{2e\mathbf{A}}{c}) = \frac{1}{m^*}(\hbar\nabla\phi' - \frac{2e\mathbf{A}}{c}),$$
(14)

where ϕ' is the phase of the LG wavefunction. The total flux enclosed by the loop is

$$\Phi = \int_{\text{loop}} \mathbf{A} \cdot d\mathbf{s} = \int_{\text{sc}} \mathbf{A} \cdot d\mathbf{s} + \int_{\text{jn}} \mathbf{A} \cdot d\mathbf{s} = \int_{\text{sc}} \frac{\Phi_0}{2\pi}(\nabla\phi' - \frac{m^*\mathbf{v}_s}{\hbar}) \cdot d\mathbf{s} + \int_{\text{jn}} \mathbf{A} \cdot d\mathbf{s},$$
(15)

where the subscripts in the integration "sc" and "jn" indicate the contours across the superconductor and the junction respectively. If the superconductor is thicker than the penetration depth, $\mathbf{v}_s$ is zero inside the superconductor, and, noting the single-valuedness (modulo 2π) of the phase, we get

$$\Phi = -\frac{\Phi_0}{2\pi}\left(\int_{\text{jn}} \nabla\phi' d\mathbf{s} + 2n\pi\right) + \int_{\text{jn}} \mathbf{A} \cdot d\mathbf{s} = -\frac{\Phi_0}{2\pi}(\gamma + 2n\pi),$$
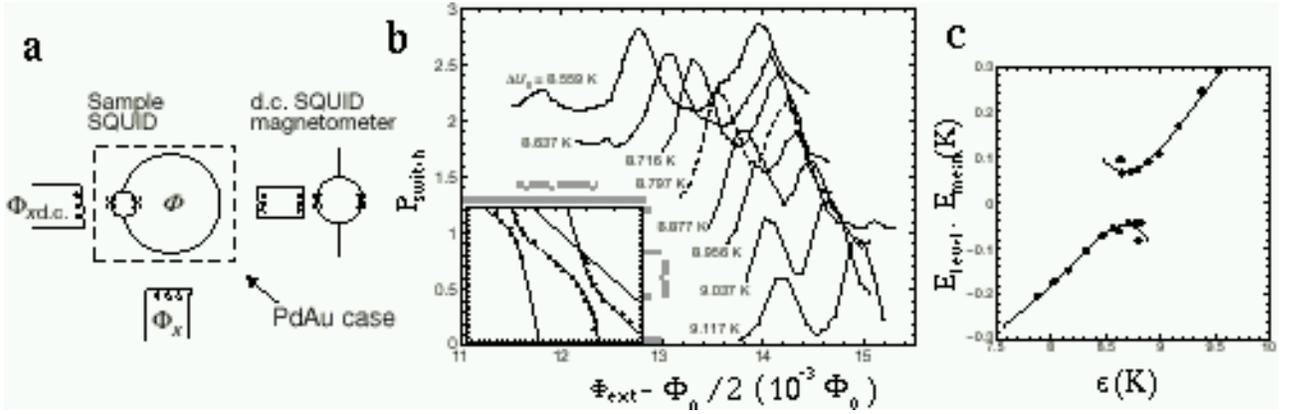(16)

6

FIG. 5: The Stony Brook Experiment.

where we have used the definition of the gauge-invariant phase difference γ, which now becomes $\gamma = 2\pi\Phi/\Phi_0 + 2n\pi$. If there are several junctions (see e.g. Fig. 4c) in a superconducting loop (this kind of device is usually called superconducting quantum interferace device, SQUID, for short), the above relation is easily generalized to

$$\sum_i \gamma_i = 2\pi\frac{\Phi}{\Phi_0} + 2n\pi, \tag{17}$$

where γ_i is the gauge-invariance phase difference across the i-th junction.

The Josephson tunneling term to the energy of the one-junction SQUID is then $-E_J\cos(2\pi\Phi/\Phi_0)$. Since the geometry is a loop, the system Hamiltonian also contains a term associated with self-inductance L, i.e. $LI_s^2/2$. The total flux contains, in addition to the externally applied flux Φ_{ext}, the term due to self-inductance, LI_s, and it is therefore $LI_s^2/2 = (\Phi - \Phi_{\text{ext}})^2/(2L)$. Including the charging energy $Q^2/(2C_J)$ as well, we arrive at the Hamiltonian of the superconducting loop with a junction

$$\mathcal{H} = -E_J\cos\left(2\pi\frac{\Phi}{\Phi_0}\right) + \frac{(\Phi - \Phi_{\text{ext}})^2}{2L} + \frac{Q^2}{2C_J} = U(\Phi) + \frac{Q^2}{2C_J}, \tag{18}$$

where $Q = -i\hbar\partial/\partial\Phi$ is the canonically conjugate variable to Φ just as momentum $\hat{p}$ to position $\hat{x}$, and

$$U(\Phi) \equiv U_0\left[\frac{1}{2}\left(\frac{2\pi(\Phi - \Phi_{\text{ext}})}{\Phi_0}\right)^2 - \beta_L\cos\left(2\pi\frac{\Phi}{\Phi_0}\right)\right], \tag{19}$$

where $U_0 \equiv \Phi_0^2/4\pi^2 L$ and $\beta_L \equiv E_J/U_0$.

In Figs. 4ef, we plot the potential for different values of Φ_{ext} (near $\Phi_0/2$) and β_L. As can be seen from the figures, the barrier height between the two lowest minima depends strongly on β_L and weakly on Φ_{ext}. As β_L increases, the barrier height increases. We remark that in order to have a double-well structure near $\Phi = \Phi_0/2$, β_L needs to be larger than unity. When temperature is low enough, only the lowest state within each well is relevant. We denote the two localized states by $|\psi_L\rangle$ and $|\psi_R\rangle$ respectively. Then the Hamiltonian is approximately two-level, and when written in terms of matrix, it is

$$\mathcal{H} \approx \begin{pmatrix} \langle\psi_L|\mathcal{H}|\psi_L\rangle & \langle\psi_L|\mathcal{H}|\psi_R\rangle \\ \langle\psi_R|\mathcal{H}|\psi_L\rangle & \langle\psi_R|\mathcal{H}|\psi_R\rangle \end{pmatrix} = \begin{pmatrix} \varepsilon_L & \Delta \\ \Delta & \varepsilon_R \end{pmatrix} \equiv -\frac{1}{2}B_z\sigma_z - \frac{1}{2}B_x\sigma_x, \tag{20}$$

where we have dropped a constant term $(\varepsilon_L + \varepsilon_R)/2$ in the last equality. $B_z = (\langle\psi_R|\mathcal{H}|\psi_R\rangle - \langle\psi_L|\mathcal{H}|\psi_L\rangle$ characterizes the asymmetry of the double well, and it depends strongly on Φ_{ext} ($B_z = 0$ when $\Phi_{\text{ext}}/\Phi_0 = 0.5$, $B_z > 0$ when $\Phi_{\text{ext}}/\Phi_0 < 0.5$, and $B_z < 0$ when $\Phi_{\text{ext}}/\Phi_0 > 0.5$ and weakly on β_L;

$B_x = 2\langle\psi_L|\mathcal{H}|\psi_R\rangle$ (which is real since $|\psi_L\rangle$ and $|\psi_R\rangle$ are local ground states hence can be taken to be real) describes tunneling between the two wells and depends on the barrier height, hence strongly on β_L and weakly on Φ_{ext} (near $\Phi_0/2$).

In order to gain more control over B_z and B_x, we can relace the Josephson junction by a smaller loop with two junctions with flux $\tilde{\Phi}_x$ threaded through; see Figs. 4bd. If the self-conductance of the loop is low, we simply replace $-E_J \cos\left(2\pi\Phi/\Phi_0\right)$ by

$$-E_J \cos\left(2\pi\Phi/\Phi_0 + \pi\tilde{\Phi}_x/\Phi_0\right) - E_J \cos\left(2\pi\Phi/\Phi_0 - \pi\tilde{\Phi}_x/\Phi_0\right) = -2E_J \cos\left(\pi\tilde{\Phi}_x/\Phi_0\right). \tag{21}$$

The result is to replace E_J by an effective $\tilde{E}_J = 2E_J \cos\left(\pi\tilde{\Phi}_x/\Phi_0\right)$. Thus, B_x and B_z can be controlled by $\tilde{\Phi}_x$ and Φ_{ext}. We remark that, in contrast to the charge qubit case, here, the dependence of B_x and B_z on $\tilde{\Phi}_x$ and Φ_{ext} is, in general, very complicated and needs to be calculated by, e.g., the WKB approximation, which we do not address here.

A. The Stony Brook Experiment

The experiment of the group at Stony Brook did not demonstrate the control of a qubit, but instead probed the superposition of two excited states (rather than the lowest two states) close to but still below the top of the barrier of the double-well[8], for if the barrier is too high, the mixing between the lowest two stateswill be exponentially suppressed. If the two excited states (denoted by $|0\rangle$ and $|1\rangle$ respectively) have the same energy when $\Phi_{\text{ext}}/\Phi_0 = 1/2$, the two energy eigenstates (within the Hilbert subspace spanned by $|0\rangle$ and $|1\rangle$) will be symmetric and antisymmetric superpositions of $|0\rangle$ and $|1\rangle$. For small deviation from that degeneracy point, the energy separation of the two eigenstates in the subspace will have the form $E = \sqrt{\varepsilon^2 + \Delta^2}$, provided the decay of excited states into lower levels can be ignored within the measuring time (so that we can ignore the broadening of the energy levels). The quantity ε is now the asymmetry of the two excited states from degeneracy, and can be controlled by $\tilde{\Phi}_x$. Δ is the mixing between these two states and can be controlled by Φ_{ext}.

The experimental setup is shown in Fig. 5a, with parameters $L = 240$ pH, $\beta_L = 2.33$, $E_c \equiv e^2/2C = 9.0$mK, $E_L \equiv \Phi_0^2/2L = 645$K, and $E_J = 2\pi L I_c/\Phi_0 = 76$K. For a given value of barrier height ΔU_0 (at degeneracy point) and externally applied flux Φ_{ext}, they prepare the system in the lowest state $|i\rangle$ at the left well, shine a milisecond pulse of 96GHz microwave onto the sample, and use a dc-SQUID to measure the change of flux state of the sample after microwave pulse is off. If the energy of $|i\rangle$ plus photon matches that of either one of the two excited states, denoted by $|0\rangle$ and $|1\rangle$, the photon will be absorbed. Due to mixing, the system can now make a interwell transition, which can be detected by the dc-SQUID. They vary the value of Φ_{ext} and determine the probability of interwell transition P_{switch} as a function of external flux Φ_{ext}; see Fig. 5b for experimental data. They repeat the whole procedure for different values of barrier height. They verify the energy-level anticrossing, which is an indication of symmetric and anti-symmetric superpositions of the two excited states at degenerate point; see Fig. 5c. They also estimate the two states differ in flux by more than $\Phi_0/4$ and in current by 2-3μA, which, in their experimental setup, corresponds to magnetic moment of order $10^{10}\mu_B$. Hence, they have demonstrated a superposition of macroscopically different states.

B. The Deft experiment

They use a low-self-conductance (L so small that we can neglect the contribution from $1/2LI^2$, and $\Phi \approx \Phi_{\text{ext}}$) superconducting loop with three junctions [9], two having the same E_J and the third one E_J'.From Eq. 17, we have

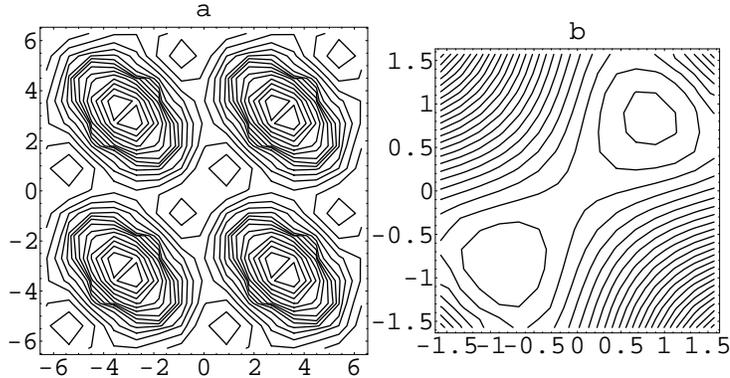$$\gamma_1 + \gamma_2 + \gamma_3 = 2\pi\Phi_{\text{ext}}/\Phi_0 \tag{22}$$

FIG. 6: The contour plot of $U(\gamma_1, \gamma_2)$ as in Eq. (21) with $E'_J/E_J = 0.75$ and $\Phi_{\text{ext}}/\Phi_0 = 0.495$.

Thus the "potential" energy term becomes

$$U = -E_J \cos \gamma_1 - E_J \cos \gamma_2 - E'_J \cos(2\pi \Phi_{\text{ext}}/\Phi_0 - \gamma_1 - \gamma_2). \qquad (23)$$

We plot the potential contours in Fig. 6 with $\Phi_{\text{ext}}/\Phi_0 = 0.495$ and $E'_J/E_J = 0.75$. We see that $U(\gamma_1, \gamma_2)$ is periodic in 2π and that there is a double-well in a small neighborhood of $(0,0)$. Again, in the experiment of the Deft group, they demonstrated the anti-crossing of the energy level of this approximate two-level system.

Fig. 7a shows the experimental setup: a three-junction SQUID sample measured by a dc-SQUID with bias current (I_{bias}) flowing through. The energy levels near half flux quantum is shown in Fig. 7b. At a fixed frequency of the microwave applied to the sample, they ramp the bias current through the dc-SQUID, in which the circulating current produces a flux through the inner loop, and measure the switching current I_{sw}, at which a voltage V builds up across the bias current flow in the dc-SQUID. The microwave induces transition between the two levels in the two wells, and a peak or dip in the switching current indicates such transition; see Fig. 7c. They confirm the level anticrossing as shown in the plot of resonance microwave frequency versus the difference of external fluxes at resonance; see Fig. 7d. The two states in their experiment differ in flux by $10^{-3}\Phi_0$, which corresponds to a magnetic moment of order $10^4 - 10^5 \mu_B$.

We emphasize again that the fact that B_z can be controlled by $\tilde{\Phi}_x$ and B_x by Φ_{ext} is valid in the neighborhood of the degeneracy point, and B_z and B_x depend, in general, on both $\tilde{\Phi}_x$ and Φ_{ext}, which makes the manipulation of single flux qubit over a broad range of control parameters more intricate than of single charge qubit.

V. A HYBRID DESIGN AND EXPERIMENT

The Quantronics Group in France recently develops a hybrid design [10] of superconducting qubit by combining the designs of charge and flux qubits, as can be seen from the central part of Fig. 8 that the left half of the circuit consists of a Cooper pair box connected two a three-junction flux qubit on the right half. They call the qubit part "quantronium". Also shown in the figure are the preparation and readout devices. They demonstrate that the ratio of decoherence time to single gate operation time is about 8,000, which is of the same order as the minimum threshold 10^4 required in order for quantum error correction to work [11].
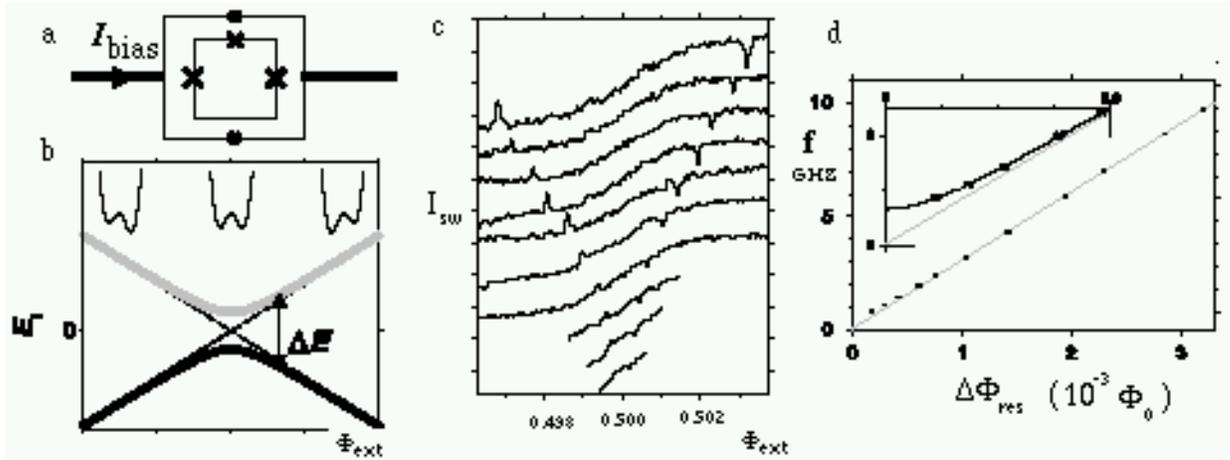
9

FIG. 7: The Delft experiment.

In their experiment, the Josephson coupling energy is of the same order of charging energy, $E_J \cong E_C$, and neither the pair number n nor the phase Θ is a good quantum number. Their sample operates at an intermediate regime, and the approximation that we use to derive the approximate two-level Hamiltonian in charge qubits does not apply here. However, when the temperature is low enough and the superconductor gap energy is the largest energy scale, the system is suitably described by the few lowest states. But how many lowest states should be kept certainly depends on the detail of energy splittings. If the condition is such that the lowest two states, denoted by $|0\rangle$ and $|1\rangle$ respectively, are sufficient (as is assumed here in the experiment), the resulting truncated Hamiltonian will be equvialent to that of a spin-1/2 system.

FIG. 8: Quantronium: a hybrid design of qubit.

Despite the unjustified assumption, they observe microwave induced oscillations (usually called Rabi oscillations) between the two levels and Ramsey fringe (which tells us the coherence time T_ϕ); see Fig. 9. Their results indicate they can perform 8000 coherent free precession turns within a period of T_ϕ.

VI. CONCLUDING REMARKS

The most important and most difficult task in realizing quantum information processing is to overcome decoherence. There are many contributions of decoherence. First of all, since the superconducting qubits we've discussed so far are only approximate two-level systems, coupling to higher level causes the leakage of information from the approximate two-level subspace. It will be interesting and of great importance to know the quantitative working conditions for experimental parameters such that the errors can still be tolerated within the technique of quantum error correction. Much more complicated contributions come from coupling to the environment. Charge qubits are susceptible to fluctuations from the voltage sources, fluctuations of the externally controlled flux, background charge noise, and measurement backaction. On the other hand, flux qubits are susceptible to background magnetic field fluctuations, nuclear spins in the substrate, unwanted magnetic dipole-dipole coupling, fluctuations in the external flux-supplying circuit, and measurement backaction. Identify-
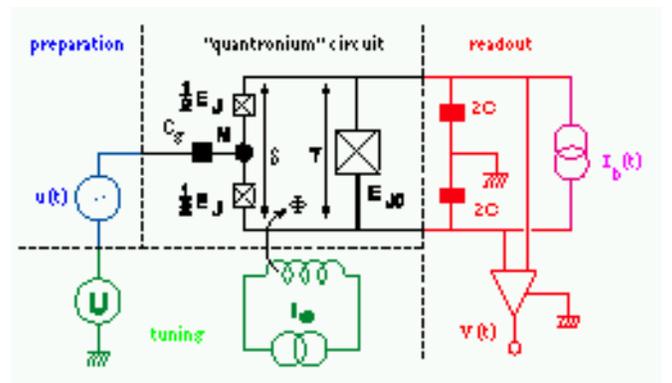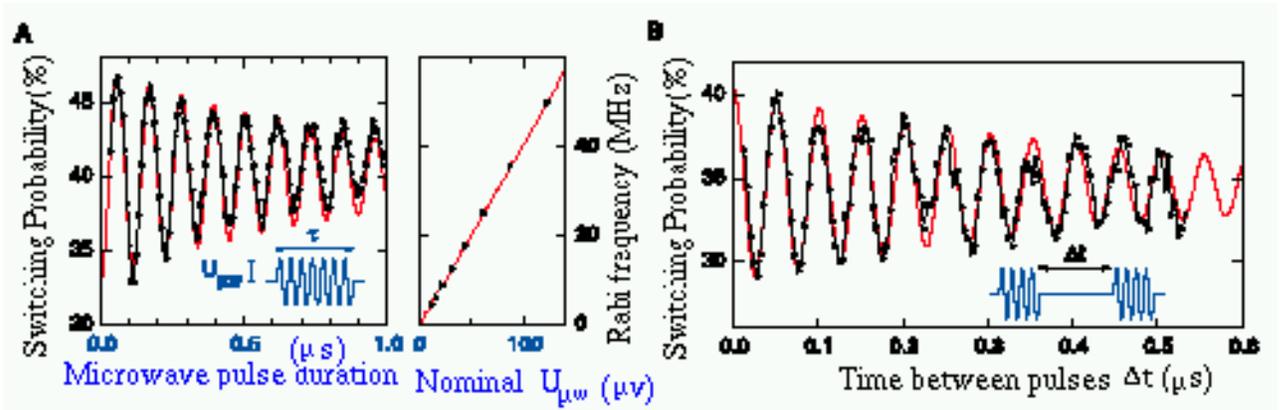
FIG. 9: The Quantronics group's experimental results: (a) Rabi oscillations (b) The Ramsey fringe experiment.

ing, analysizing, and reducing the dominant dephasing effects will be a crucial step toward quantum computation[12].

The measurement device is itself a quantum mechanical system, which couples to the quantum bits under study. This process should be described by quantum mechanics itself. For the purpose of state readout, the measuring apparatus, after coupling with the qubit for a certain duration, should be able to tell us the information about the state. This reflects in the probability evolution that there should be a period of time, in which there are two distinct peaks. For more detail, see, e.g., Ref. [12] for the case of a single electron transistor used to readout a charge qubit.

We have seen, in this Paper, several proposals for designing superconducting qubits and some verifications and demonstrations for the coherent superposition and control of single qubit states. The next exciting step is to demonstrate the controllability of two-qubit operations. Several schemes for coupling charge and flux qubits have been proposed [12–14]. Conceivably, theoretical analysis of decoherence and optimal coupling schemes and experimental realization of controllable inter-qubit interactions will be more difficult than those of single qubit, and require more thorough investigation. Achieving controlled inter-qubit operations will be a huge step torward realizing quantum computers.

[1] D. P. DiVincenzo, Science **270**, 255 (1995).

[2] S. Lloyd, Sci. Am. **273**, 44 (1995).

[3] D. P. DiVincenzo, quant-ph/0002077.

[4] A. J. Leggett, Contemp. Phys. **25**, 583 (1984).

[5] Y. Nakamura, Y. A. Pashkin, and J. S. Tsai, Nature **398**, 786 (1999).

[6] Y. Nakamura, C. D. Chen, and J. S. Tsai, Phys. Rev. Lett. **79**, 2328 (1997).

[7] Y. Nakamura, Y. A. Pashkin, T. Yamamoto, and J. S. Tsai, Phys. Rev. Lett. **88**, 047901 (2002).

[8] J. R. Frieman, V. Patel, W. Chen, S. K. Tolpygo, and J. E. Lukens, Nature **406**, 43 (2000).

[9] C. H. van der Wal, A. C. J. ter Haar, F. K. Wilhelm, R. N. Schouten, C. J. P. M. Harmans, T. P. Orlando, S. Lloyd, and J. E. Mooij, Science **290**, 773 (2000).

[10] D. Vion, A. Aassime, A. Cottet, P. Joyez, H. Pothier, C. Urbina, D. Esteve, and M. H. Devoret, Science **296**, 886 (2002).

[11] J. Preskill, J. Proc. R. Soc. London Ser. A **545**, 385 (1998).

[12] Y. Makhlin, G. Schön, and A. Shnirman, Rev. Mod. Phys. **73**, 357 (2001).

[13] J. E. Mooij, T. P. Orlando, L. Levitov, L. Tian, C. H. van der Wal, and S. Lloyd, Science **285**, 1036 (1999).

11

[14] Y. Makhlin, G. Schön, and A. Shnirman, Nature **398**, 305 (1999).

[15] The formalism of this Paper is mostly based on Ref. [12].

[16] See M. Tinkham, *Introduction to Superconductivity* (McGraw-Hill, New York, ed. 2, 1996), chapters 6 and 7.

[17] In general, this energy depends on the process of tunneling. But, here, the electrons can only tunnel through the Josephson junction. See Tinkham.